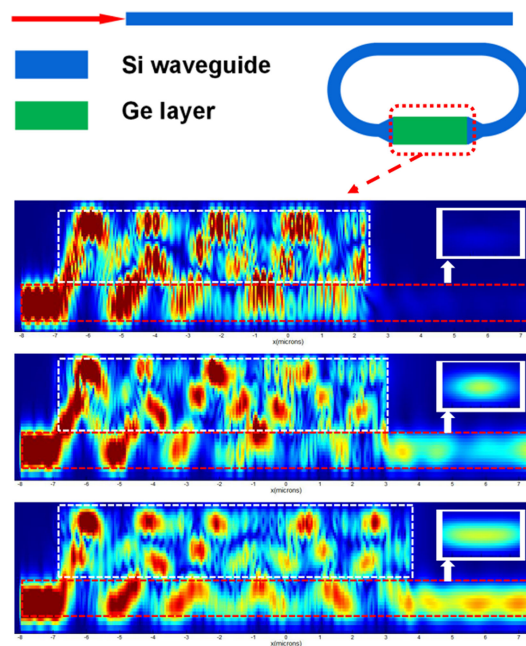


High-Performance Microring Resonator Ge-on-Si Photodetectors by Optimizing Absorption Layer Length

Volume 12, Number 4, August 2020

Jishi Cui
Tiantian Li
Hongmin Chen
Wenjing Cui



DOI: 10.1109/JPHOT.2020.3010502

High-Performance Microring Resonator Ge-on-Si Photodetectors by Optimizing Absorption Layer Length

Jishi Cui¹, Tiantian Li,² Hongmin Chen,¹ and Wenjing Cui¹

¹School of Information Engineering, Sanming University, Sanming 365004, China

²State Key Laboratory of Transient Optics and Photonics, Xi'an Institute of Optics and Precision Mechanics (XIOPM), Chinese Academy of Science (CAS), Xi'an 710119, China

DOI:10.1109/JPHOT.2020.3010502

This work is licensed under a Creative Commons Attribution 4.0 License. For more information, see <https://creativecommons.org/licenses/by/4.0/>

Manuscript received June 8, 2020; revised July 10, 2020; accepted July 15, 2020. Date of publication July 21, 2020; date of current version August 3, 2020. This work was supported in part by State Key Laboratory of Advanced Optical Communication Systems and Networks, China, in part by Digital Fujian Research Institute for Industrial Energy Big Data, in part by Fujian Province University Key Laboratory for the Analysis and Application of Industry Big Data, in part by Fujian Key Lab of Agriculture IOT Application, and in part by IOT Application Engineering Research Center of Fujian Province Colleges and Universities. Corresponding author: Jishi Cui (email: jscui@fjsmu.edu.cn).

Abstract: We studied the relationship between the absorption layer length and the performance of Ge-on-Si microring resonator photodetectors. The principle of optimizing the absorption layer length based on the light field distribution was proposed. In the Ge-on-Si photodetectors, the transmission light field is alternately distributed among the germanium absorption layer and the silicon waveguide layer, and gradually absorbed by the germanium layer. For the Ge-on-Si microring resonator photodetectors, the length of the germanium absorption layer should be set to achieve the maximum light field distribution in the silicon layer at the end of the photodetector, then the remaining optical power can be coupled back to the silicon waveguide and transmit in the microring for absorption again. We demonstrated by simulation that, the device with optimized length of 11 μm has larger bandwidth, smaller dark current, and higher responsivity than the device with 14 μm absorption layer by simulation @1550nm.

Index Terms: Ge-on-Si photodetectors, silicon photonics, Integrated optoelectronics.

1. Introduction

For the optical communication and interconnect system, the photodetector is a key device for receiver part. In the early stage, the main choices are InP and InGaAs [1]–[4] since they have excellent performance. However, the III-V devices require a high cost and are not compatible with the Complementary Metal Oxide Semiconductor (CMOS) technology for large-scale integration. Silicon-based optoelectronic devices arouse an extensively research interest in recent years because of ease of integration and low cost [5]–[9]. However, the band gap of silicon is only 1.1 eV, which determines the absorption wavelength is shorter than 1100 nm and limits the application for C-band photodetectors. Considering germanium's similar crystal structures and lattice constants comparing with silicon, meanwhile the absorption limit can be extended to 1.9 μm which could cover C-band. And germanium photodetectors are compatible with CMOS technology. So the germanium photodetectors are the best choice of Si-based photodetectors. In recent years, there are many papers have reported the progress of Ge-on-Si photodetectors [10]–[17]. In the Ge-on-Si



Fig. 1. The waveguide structure diagram of the Ge-on-Si microring photodetector, in which the germanium absorption layer is on the silicon waveguide.

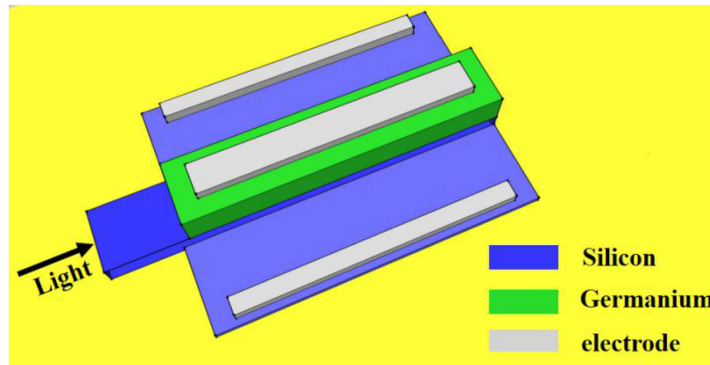


Fig. 2. The schematic diagram of the active absorption region of the microring resonator photodetector.

photodetectors' design, the short germanium absorption layer has a small capacitance and lower electrode loss, so a larger bandwidth can be realized. At the same time, the small size can achieve a lower dark current and high density integration. However, high responsivity requires a long germanium absorption layer.

The responsivity enhanced Ge-on-Si microring resonator photodetectors by increasing absorption times have been reported [18]–[21]. However, the reported improvement of the microring photodetectors' performance is still not significant, which is caused by the unoptimized length of the germanium absorption layer. If the absorption length is not optimized, most remaining optical power after the first absorption would be scattered and reflected, which is not coupled to the silicon waveguide of microring for multiple absorption.

2. Structure

A waveguide structure diagram of a microring resonator photodetector is depicted in Fig. 1. The germanium absorption layer is epitaxial growth on the silicon-on-insulator (SOI) rib waveguide. Optical power is evanescently coupled to the germanium layer from the silicon layer. This configuration ensures a good overlap of the guide mode between the germanium absorption layer and the silicon waveguide [22]. Fig. 2 is a three-dimensional structure diagram of the active region of the photodetector. The top of the germanium and part of silicon slab layer are set to be heavy doping for realizing good ohmic contact with electrode. The heavily doped of the germanium is N-type and the doping element is phosphorus, the concentration is $3 \times 10^{19} \text{ cm}^{-3}$. The heavily doped of silicon slab is P-type and the doping element is boron, the concentration is $1 \times 10^{20} \text{ cm}^{-3}$. The thickness of the slab is 90 nm. The width of the electrode is 0.5 μm , and the length varies according to germanium layer's length. The thickness of the germanium layer is 0.5 μm and the width is 6 μm . These parameters match current silicon-based optoelectronic process parameters.

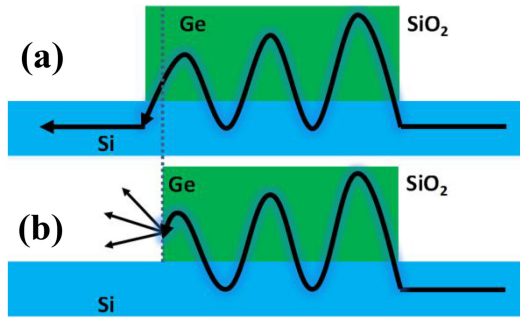


Fig. 3. The schematic diagram of the photodetectors with and without optimized Ge absorption length, (a) With an optimized germanium length, the unabsorbed light is coupled back to the silicon waveguide for transmission, (b) Without an optimized germanium length, unabsorbed light is scattered at the Ge/SiO₂ interface.

3. Light field

In the Ge-on-Si photodetectors, the light field is transmitted alternately between the silicon waveguide layer and the germanium absorption layer as an evanescent wave. Therefore, the distribution of the light field in the germanium layer and the silicon layer is periodic [23]. If the optical power is mainly distributed in the germanium layer at the end of the absorption region, most of the remaining light field energy will be scattered, reflected or incident to silicon dioxide at the Ge/SiO₂ interface, as shown in Fig. 3(b). Therefore, the unabsorbed light will not be further absorbed through the micro-ring waveguide. It does not contribute to the responsivity. On the contrary, if the light field is maximum in the silicon layer at the end of the absorption region, most of the remaining light field energy will be coupled back to the silicon waveguide in microring for transmission multiple absorption, as shown in Fig. 3(a). In this case, the responsivity of the photodetector can be improved.

In order to further verify the above theory, we simulated the light field in the photodetector by FDTD (finite-difference time-domain) as shown in Fig. 4 with the wavelength of the input light is 1550nm. According to the characteristics of the light field distribution, we selected three photodetectors with the absorption length of 9.3 μm, 10 μm and 10.7 μm. The distribution of light field among the silicon waveguide and the germanium layer in the Ge-on-Si photodetector with different absorption layer length are shown in Fig. 4. In the silicon waveguide at the end of the photodetector, the light energy of the 9.3 μm length photodetector is less than the 10.7 μm length photodetector, although it has a higher unabsorbed light energy, which is shown in the insets. This is because in the 9.3 μm length photodetector, most of the remaining light energy is scattered at the Ge/SiO₂ interface. In the 10.7 μm length photodetector, most of the remaining light energy is coupled back to the silicon waveguide to transmission for absorbing multiple times. The light transmission in 9.3 μm length photodetector as Fig. 4(a) and in 10.7 μm as Fig. 4(c). The state of the 10 μm length photodetector is somewhere in between, as a reference.

4. Responsivity

We studied the relationship between the absorption length and the responsivity of the microring resonator photodetector as shown in Fig. 5. When the thickness of the absorption layer is larger than 0.5 μm and the width is larger than 2 μm, the light field can be better confined in the absorption layer. So the light absorption of the electrode is very weak and the responsivity will not increase as the width and thickness increase continuously. The lattice mismatch of Ge/Si will cause tensile stress in the germanium layer at the heterojunction and cause the refractive index decreased. As the length of the germanium layer increases, the responsivity of microring resonator photodetectors increase periodically, which is monotonical in the case of straight waveguide

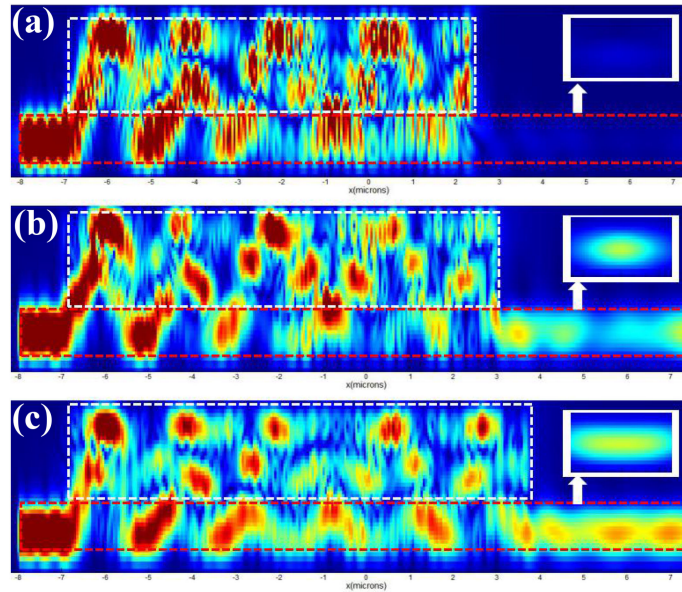


Fig. 4. The light field distribution along the light transmission direction of photodetectors with germanium layer length of (a) $9.3\ \mu\text{m}$, (b) $10\ \mu\text{m}$, and (c) $10.7\ \mu\text{m}$. The red dashed boxes indicates the silicon waveguides, the white dashed boxes are the germanium layers. The insets are the light field energy distribution perpendicular to the light transmission direction of the silicon waveguide at the back end of the photodetectors. The reference light field energy scale is the same for all the light field simulation.

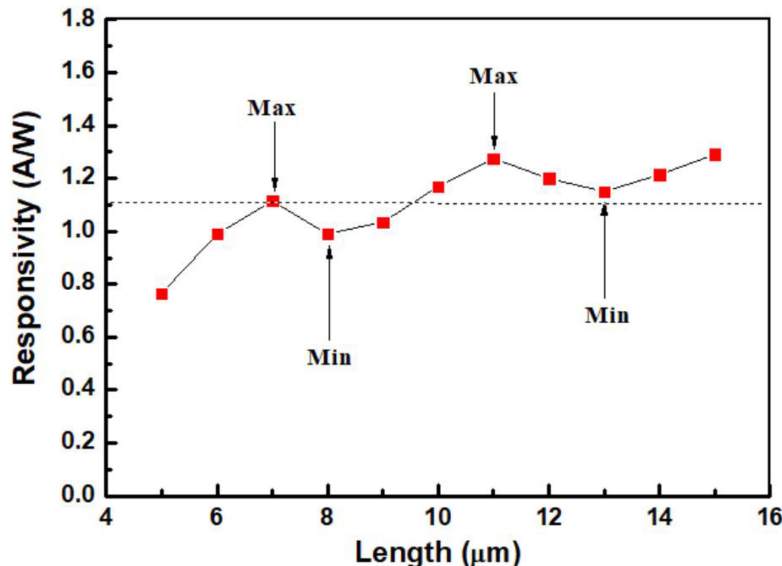


Fig. 5. The responsivity of photodetectors with different germanium layer length.

photodetector. Due to uneven light field distribution of evanescent wave in germanium layer, the increased rates of responsivity changes with length. The responsivity of the microring resonator photodetector increasing periodically with length is mainly caused by the multiple absorption by the microring structure. The maximum value of responsivity is achieved when the unabsorbed light is mostly coupled back to the silicon waveguide to transmission and for absorbed multiple times, like Fig. 4(c). On the contrary, the minimum value of responsivity is achieved when the

unabsorbed light is scattered at the end of the photodetector, so it cannot be coupled back to the silicon waveguide in the microring to be transmitted and absorbed multiple times, as shown in Fig. 4(a). The maximum value points of the responsivity are realized when the length are $7 \mu\text{m}$ and $11 \mu\text{m}$, the minimum value points of the responsivity are realized when the length are $8 \mu\text{m}$ and $13 \mu\text{m}$. This shows that a photodetector with a shorter absorption length can get higher responsivity than a photodetector with a longer absorption length. The period in which the responsivity changes with the length is consistent with the period in which the light field is alternately distributed in the Ge/Si heterojunction. Therefore, the designing of the length of a microring resonator photodetector should be based on the characteristics of the evanescent wave field distribution. In this way, the length of the germanium absorption layer can be shortened to increase the bandwidth and reduce the dark current, meanwhile increase the responsivity.

5. Bandwidth

The bandwidth is also a relevant index of the size of the photodetectors. In theory, 3 dB bandwidth is determined by the RC constant, carrier transit time, and electrode length. The carrier transport time mainly depends on the thickness of the germanium absorption layer which can be described by [24], [25]:

$$f_{tr} = \frac{0.45v_h}{d}, \quad (1)$$

Where d is the thickness of the intrinsic germanium film, and v_h is the hole saturation drift velocity of germanium. The length and width mainly determine the capacitance, resistance and electrode of the photodetector. The influence of its capacitance and resistance in the 3dB bandwidth of the photodetector can be expressed as:

$$f_{RC} = \frac{1}{2\pi RC}, \quad (2)$$

where R is the load resistance, C is the capacitance. 3 dB bandwidth of the photodetector is determined by the above factors, which can be calculated by the following formula:

$$f_{3dB} = \frac{1}{\sqrt{f_{tr}^{-2} + f_{RC}^{-2}}}. \quad (3)$$

According to the transmission line effect, the longer electrode increases the signal loss. When the length of the photodetector increases, the capacitance and the transmission line loss will be increased, then result in the reduction of 3dB bandwidth. Therefore, to obtain a large 3dB bandwidth, a short photodetector length is required.

The multiple absorption of the light will also affect the 3dB bandwidth of the microring resonator photodetectors. Because the remaining light energy after second absorption is very low, we mainly consider the effect of second absorption on the bandwidth. The effect is mainly due to the time loss caused by the remaining light transmission. Because the transmission rate of light is much greater than the transmission rate of carriers, so the second absorption duration for the microring resonator photodetectors with $60 \mu\text{m}$ silicon waveguide is just 2.04 ps, corresponding to the frequency of 0.49 THz. This is much greater than the frequency ($\leq 80 \text{ GHz}$) of PN junctions ($\geq 5 \mu\text{m}$), so in this case the effect of the second absorption on the 3 dB bandwidth is very small. The photodetector is longer, the influence of the second absorption on the 3 dB bandwidth is smaller. Fig. 6 is a simulation result of a photodetector's 3dB bandwidth changing with length ($5 \mu\text{m} \leq L \leq 15 \mu\text{m}$).

6. Dark Current

The dark current-voltage (I-V) characteristic curves at -1V of the photodetectors are shown in Fig. 6. In PIN photodetectors, the dark current includes the surface dark current and bulk dark

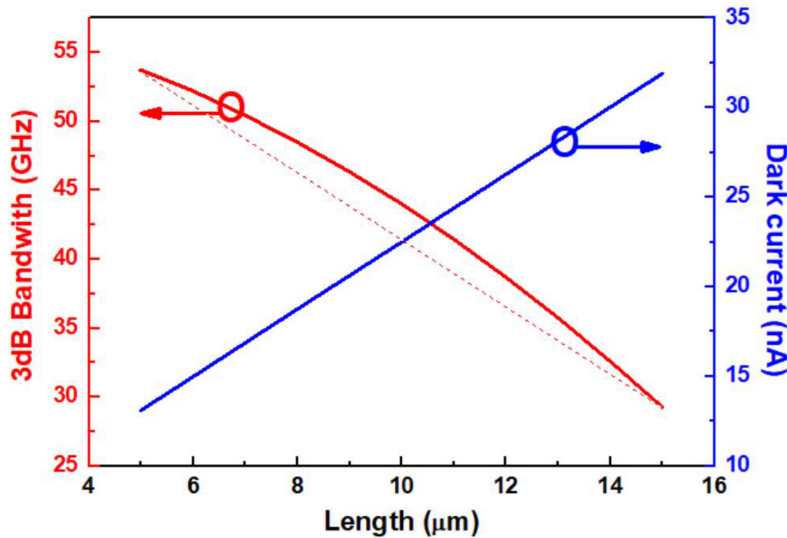


Fig. 6. The 3dB bandwith and dark current of photodetectors with different absorption length.

current, which can be calculated by the following equation [26]:

$$I = J_{\text{sur}} \cdot 2(W + L) + J_{\text{bulk}} \cdot W \cdot L \quad (4)$$

where L is the length, W is the width of the germanium layer. The main factor of dark current is the recombination center generated by defects. In the surface, the defects mainly come from dangling bonds. Dangling bonds will form high-density defects, and the defects will play the role of recombination centers, and will recapture electrons and holes to recombine at the defect energy level, thereby generating dark current [27]–[29]. Inside the germanium material, the recombination center is mainly caused by point defects and dislocation defects. For a mature germanium epitaxial growth process, the density of internal defects in the material is much smaller than the density of dangling bonds on the surface. Therefore, the surface dark current density is much greater than the bulk dark current density. In the case of a certain process and its size is not smaller than the feature size, the dark current depends on the size of the device. The photodetector with a short germanium layer will have a low dark current. We take the classical values of the current density from [11], J_{sur} as 0.31 mA / cm and J_{bulk} as 0.21 mA / cm² under the bias of -1V. The dark current of Ge-on-Si microring resonator photodetectors with different lengths was calculated as shown in Fig. 6. For every 1 μm increase in its length, the dark current will increase by 1.88 nA. Therefore, reducing the size of the photodetector can reduce the dark current effectively. The surface dark current density and the bulk dark current density are different under different processes, but the relationship between the size and size of the total dark current is certain, like equation (4).

7. Summary

In this paper, we proposed a design principle for a microring resonator photodetector based on the characteristics of the light field distribution in the Ge-on-Si photodetector. The characteristics of the light field distribution were revealed by FDTD simulation. The responsivity, 3 dB bandwidth, and dark current of the photodetector in the length range of 5 μm–15 μm were simulated and calculated. The results show that, unlike traditional straight waveguide photodetectors, the responsivity of microring resonator photodetector does not increase monotonically with the length increase, which is depend on the multiple absorption of the remaining light after first absorption. For 3 dB bandwidth and dark current, the microring resonator photodetector and the straight waveguide photodetector show the similar characteristics. The 3 dB bandwidth decreases and the dark current increases

TABLE 1
Characteristics of the Photodetectors With Different Length

Length (μm)	5	6	7	8	9	10	11	12	13	14	15
Responsivity (A/W)	0.51	0.63	0.71	0.66	0.69	0.83	0.92	0.85	0.81	0.86	0.93
3dB bandwith (GHz)	53.75	52.20	50.45	48.50	46.35	44.00	41.45	38.70	35.75	32.60	29.25
Dark current (nA)	13.12	15.00	16.88	18.76	20.64	22.52	24.40	26.28	28.16	30.04	31.92

with the length increases. This provides an effective reference for the design of Ge-on-Si microring photodetectors. The parameter changes with the length of the photodetector are shown in the Table 1.

References

- [1] J. Wang *et al.*, "Highly polarized photoluminescence and photodetection from single indium phosphide nanowires," *Science*, vol. 293, no. 5534, pp. 1455–1457, 2001.
- [2] M. Razeghi *et al.*, "A high quantum efficiency GaInAs-InP photodetector-on-silicon substrate," *J. Appl. Phys.*, vol. 65, no. 10, pp. 4066–4068, 1989.
- [3] X. Duan, Y. Huang, X. Ren, Y. Shang, X. Fan, and F. Hu, "High-efficiency InGaAs/InP photodetector incorporating SOI-based concentric circular subwavelength gratings," *IEEE Photon. Technol. Lett.*, vol. 24, no. 10, pp. 863–865, May 2012.
- [4] G. Roelkens *et al.*, "Laser emission and photodetection in an InP/InGaAsP layer integrated on and coupled to a Silicon-on-Insulator waveguide circuit," *Opt. Express*, vol. 14, no. 18, pp. 8154–8159, 2006.
- [5] M. Asghari and A. V. Krishnamoorthy, "Silicon photonics: Energy-efficient communication," *Nature Photon.*, vol. 5, no. 5, pp. 268–270, 2011.
- [6] H. Shu, B. Shen, Q. Deng, M. Jin, X. Wang, and Z. Zhou, "A design guideline for mode (DE) Multiplexer based on integrated tapered asymmetric directional coupler," *IEEE Photon. J.*, vol. 11, no. 5, pp. 1–12, Oct. 2019.
- [7] Y. A. Vlasov *et al.*, "On-chip natural assembly of silicon photonic bandgap crystals," *Nature*, vol. 414, no. 6861, pp. 289–293, 2001.
- [8] S. Faralli, G. Meloni, F. Gambini, J. Klamkin, L. Potì, and G. Contestabile, "A compact silicon coherent receiver without waveguide crossing," *IEEE Photon. J.*, vol. 7, no. 4, pp. 1–6, Aug. 2015.
- [9] L. Feng *et al.*, "Nonreciprocal light propagation in a silicon photonic circuit," *Science*, vol. 333, no. 6043, pp. 729–733, 2011.
- [10] J. Michel, J. Liu, and L. C. Kimerling, "High-performance Ge-on-Si photodetectors," *Nature Photon.*, vol. 4, no. 8, pp. 527–534, 2010.
- [11] J. Cui and Z. Zhou, "High-performance Ge-on-Si photodetector with optimized DBR location," *Opt. Lett.*, vol. 42, no. 24, pp. 5141–5144, 2017.
- [12] J. Cui *et al.*, "Optical saturation characteristics of dual-and single-injection Ge-on-Si photodetectors," *Chin. Opt. Lett.*, vol. 16, no. 7, 2018, Art. no. 072502.
- [13] X. Hai-Yun *et al.*, "Zero biased Ge-on-Si photodetector with a bandwidth of 4.72 GHz at 1550 nm," *Chin. Phys. B*, vol. 18, no. 6, 2009, Art. no. 2542.
- [14] Q. Fang *et al.*, "Demonstration of a vertical pin Ge-on-Si photo-detector on a wet-etched Si recess," *Opt. Express*, vol. 21, no. 20, pp. 23325–23330, 2013.
- [15] M. J. Byrd *et al.*, "Mode-evolution-based coupler for high saturation power Ge-on-Si photodetectors," *Opt. Lett.*, vol. 42, no. 4, pp. 851–854, 2017.
- [16] N. K. Hon *et al.*, "Design and performance of high-speed Ge-on-Si waveguide photodiodes," in *Proc. 2017 IEEE 14th Int. Conf. Group IV Photon.*, 2017, pp. 177–178.
- [17] N. J. D. Martinez *et al.*, "Single photon detection in a waveguide-coupled Ge-on-Si lateral avalanche photodiode," *Opt. Express*, vol. 25, no. 14, pp. 16130–16139, 2017.
- [18] J. Song *et al.*, "A microring resonator photodetector for enhancement in L-band performance," *Opt. Express*, vol. 22, no. 22, pp. 26976–26984, 2014.
- [19] O. I. Dosunmu, D. D. Cannon, M. K. Emsley, L. C. Kimerling, and M. S. Unlu, "High-speed resonant cavity enhanced Ge photodetectors on reflecting Si substrates for 1550-nm operation," *IEEE Photon. Technol. Lett.*, vol. 17, no. 1, pp. 175–177 Jan. 2005.
- [20] K. C. Balram, R. M. Audet, and D. A. B. Miller, "Nanoscale resonant-cavity-enhanced germanium photodetectors with lithographically defined spectral response for improved performance at telecommunications wavelengths," *Opt. Express*, vol. 21, no. 8, pp. 10228–10233, 2013.

- [21] O. I. Dosunmu *et al.*, "Resonant cavity enhanced Ge photodetectors for 1550 nm operation on reflecting Si substrates," *IEEE J. Sel. Topics Quantum Electron.*, vol. 10, no. 4, pp. 694–701, Jul./Aug. 2004.
- [22] G. Li *et al.*, "Improving CMOS-compatible Germanium photodetectors," *Opt. Express*, vol. 20, no. 24, pp. 26345–26350, 2012.
- [23] Z. Tu *et al.*, "A compact evanescently-coupled germanium PIN waveguide photodetector[C]/Nanophotonics and Micro/Nano Optics," *Soc. Opt. Photon.*, vol. 8564, 2012, Art. no. 85640X.
- [24] L. Chen and M. Lipson, "Ultra-low capacitance and high speed germanium photodetectors on silicon," *Opt. Express*, vol. 17, no. 10, pp. 7901–7906, 2009.
- [25] S. M. Sze and Ng K. K. *Physics of semiconductor devices[M]*. Hoboken, NJ, USA: Wiley, 2006.
- [26] J. H. Park and H Y. Yu, "Dark current suppression in an erbium–germanium–erbium photodetector with an asymmetric electrode area," *Opt. Lett.*, vol. 36, no. 7, 1182–1184, 2011.
- [27] M. Takenaka *et al.*, "Dark current reduction of Ge photodetector by GeO₂ surface passivation and gas-phase doping," *Opt. Express*, vol. 20, no. 8, pp. 8718–8725, 2012.
- [28] H. Chen *et al.*, "Dark current analysis in high-speed germanium pin waveguide photodetectors," *J. Appl. Phys.*, vol. 119, no. 21, 2016, Art. no. 213105.
- [29] S. Okumura *et al.*, "Study on the effects of the Si capping layer growth conditions on the leakage current of Ge photodetector," *Japanese J. Appl. Phys.*, vol. 56, no. 10, 2017, Art. no. 102201.